ISSN 1674-1056
http://cpb.iphy.ac.cn
http://iopscience.iop.org/cpb
中国物理 B
Chinese Physics
中国物理
Chinese Physics B

Review of photoinduced effect in manganite films and their heterostructures

Xin-Yu Li(李欣谕), Long Zhao(赵龙), Xiang-Yang Wei(魏向洋), Hao Li(李豪), Ke-Xin Jin(金克新)

Citation: Chin. Phys. B . 2018, 27(11): 117501. **doi:** 10.1088/1674-1056/27/11/117501

Journal homepage: http://cpb.iphy.ac.cn; http://iopscience.iop.org/cpb

What follows is a list of articles you may be interested in

Structure dependence of magnetic properties in yttrium iron garnet by metal-organic decomposition method

Yuan Liu(刘园), Xiang Wang(王翔), Jie Zhu(朱杰), Runsheng Huang(黄润生), Dongming Tang(唐东明)

Chin. Phys. B . 2017, 26(5): 057501. **doi:** 10.1088/1674-1056/26/5/057501

Size-dependent exchange bias in single phase Mn_3O_4 nanoparticles

Song-Wei Wang(王松伟), Xin Zhang(张鑫), Rong Yao(姚蓉), Guang-Hui Rao(饶光辉)

Chin. Phys. B . 2016, 25(11): 117502. **doi:** 10.1088/1674-1056/25/11/117502

Nanoscale control of low-dimensional spin structures in manganites

Jing Wang(王静), Iftikhar Ahmed Malik, Renrong Liang(梁仁荣), Wen Huang(黄文), Renkui Zheng(郑仁奎), Jinxing Zhang(张金星)

Chin. Phys. B . 2016, 25(6): 067504. **doi:** 10.1088/1674-1056/25/6/067504

Magnetic–optical bifunctional $CoPt_3$/Co multilayered nanowire arrays

Su Yi-Kun, Yan Zhi-Long, Wu Xi-Ming, Liu Huan, Ren Xiao, Yang Hai-Tao

Chin. Phys. B . 2015, 24(10): 107505. **doi:** 10.1088/1674-1056/24/10/107505

Emergent phenomena in manganites under spatial confinement

Shen Jian, T. Z. Ward, L. F. Yin

Chin. Phys. B . 2013, 22(1): 017501. **doi:** 10.1088/1674-1056/22/1/017501

TOPICAL REVIEW — 80th Anniversary of Northwestern Polytechnical University (NPU)

Review of photoinduced effect in manganite films and their heterostructures*

Xin-Yu Li(李欣谕), Long Zhao(赵龙), Xiang-Yang Wei(魏向洋), Hao Li(李豪), and Ke-Xin Jin(金克新)†

Shaanxi Key Laboratory of Condensed Matter Structures and Properties, Northwestern Polytechnical University, Xi'an 710072, *China*

(Received 18 July 2018; revised manuscript received 6 September 2018; published online 8 October 2018)

Light–matter interaction plays an important role in the non-equilibrium physics, especially in strongly correlated electron systems with complex phases. Photoinduced effect can cause the variation in the physical properties and produce some emergent phases. As a classical archetype, manganites have received much attention due to their colossal magnetoresistance (CMR) effect and the strong interaction of charge, spin, orbital, and lattice degrees of freedom. In this paper, we give an overview of photoinduced effect in manganites and their heterostructures. In particular, some materials, including ZnO, Si, $BiFeO_3$ (BFO), titanate-based oxides, and $0.7Pb(Mg_{1/3}Nb_{2/3})O_3$-$0.3PbTiO_3$ (PMN-PT) have been integrated with manganites. Heterostructures composed of these materials display some exciting and intriguing properties. We do hope that this review offers a guiding idea and more meaningful physical phenomena will be discovered in active areas of solid state physics and materials science.

Keywords: manganites, heterostructures, photoinduced effect

PACS: 75.47.Lx, 72.40.+w, 73.40.Lq **DOI:** 10.1088/1674-1056/27/11/117501

1. Introduction

As typical strongly correlated electron systems, transition-metal oxides with perovskite or related structures have presented novel physical properties and mechanisms due to the complex interplay of charge, spin, orbital, and lattice degrees of freedom. In particular, the emergent physics have attracted the interest of many scientists and continuous research upsurge, such as the cuprate superconductors,[1,2] multiferroics,[3–6] colossal magnetoresistance (CMR) effect,[7] and 2-dimensional electron gas.[8–12] Among these intriguing properties, the CMR effect has sparked a number of studies on the electromagnetic properties and the exploration of new phases. A milestone of the CMR effect is the discovery in doped perovskite-type manganites in 1993 by Helmholt *et al.*[13] The appearance of CMR effect can be qualitatively explained with Zener double exchange model,[14] the cooperative Jahn–Teller effect,[15] as well as electronic phase separations (EPS).[16] Usually, the parent $RE\mathrm{MnO_3}$ oxides (RE = trivalent rare earth element) with the perovskite type structure usually are antiferromagnetic semi-conductive or insulating. If the trivalent rare earth element is partially doped with a divalent alkaline earth element, the doped manganites $RE_{1-x}A_x\mathrm{MnO_3}$ (A = Ca, Sr, and Ba) are formed and show a variety of astonishing physical phenomena.[17,18] Meanwhile, the manganites possess versatile unconventional electromagnetic phases as a function of doping x and temperature. Thus, besides magnetic field, other external stimuli may unbalance the competing phases and can drive the dramatic phase conversion on a macroscopic scale, such as photo-irradiation,[19] x-rays,[20] electron-beams,[21] voltage effect,[22,23] and current injection.[24] The underlying mechanism is believed to be consistent with that of CMR. For example, the photo-irradiation, being the external perturbation, offers a convenient and powerful method to change the charge carriers and causes the variation in the physical properties of manganites.[25] Additionally, it also induces the appearance of some hidden phases,[26] which is promising for photonic devices and photoelectric applications.

Before proceeding, we offer readers to several earlier reviews on manganites. For examples, Dagotto[27] and Tokura[28] introduced the basic properties of perovskite manganites and the effects of doping on electronic phase diagrams as well as on transport properties in detail. Yi *et al.*[29] reviewed the magnetic phenomena at oxide interfaces. Huijben *et al.*[30] discussed the transport anisotropy controlled by the oxygen octahedral coupling. There are several reviews that focus on the structure and strain affecting transport and physical properties. Prellier *et al.*[31] and Haghiri–Gosnet *et al.*[32] focused on the effects of epitaxial strains on the physical properties of CMR manganite films. Van *et al.*[33] reviewed different methods of accommodating the strain induced by the substrate. We also would like to provide readers with the reviews of related effects and phenomena. Wang *et al.*[34] summarized the domain walls of those manganites and Zhang *et*

*Project supported by the National Natural Science Foundation of China (Grant Nos. 51572222, 50702046, 51172183, and 11604265).

†Corresponding author. E-mail: jinkx@nwpu.edu.cn

© 2018 Chinese Physical Society and IOP Publishing Ltd

al.[35] discussed the fundamental issues related to the size effects on the magnetic properties and charge ordering in manganites. Liu *et al.*[36] reviewed CMR effect in manganites and related prototype devices. Siwach *et al.*[37] summarized the potential for low-field magnetic field induced by grain boundaries. Liu *et al.*[38] presented a comprehensive review on the electronic structure, transport and magnetic properties of manganites and underlying physics. Dong *et al.*[39] focused on the competition and modulation of various phases in perovskite manganites. Ge *et al.*[40] and Wang *et al.*[41] gave a brief review of recent investigations on oxide heterostructures based on the phase separation scenario.

Researches about the properties of manganites and their heterostructures include a large field with a long history and depth, far beyond the scope of this short review. Therefore, we only provide a more comprehensive summary of the photoinduced effect and related physics. The goal is to give a clear understanding in the field of complex oxides and the optical physics of the electron strong correlation systems.

2. Photoinduced effect in manganite films

Recently, the photoinduced phase transition (PIPT) has attracted more attention, especially in CMR manganite systems with rich electronic and structural phases. In this multiple phases competition and coexistence system, the spin, charge, and orbital degrees of freedom of 3d electrons will make it possible to control the various properties of manganite via cooperative effects induced by optical excitation.[42] In addition, in laser irradiation materials, photons will trigger a collective change in electronic states. If a material has a mixed valence with localized electrons and strong electron–lattice coupling, it will be a good candidate for PIPT, just like the Mn^{3+} and Mn^{4+} in doped manganites system.[43]

Photoinduced effects in different manganite systems exhibit different phenomena caused by different mechanisms. Doped manganites have complex phase diagrams and two kinds of systems are usually focused: the charge-ordering system with EPS and the system with the typical metal–insulator transition.

2.1. Charge-ordering phase with EPS

Some photoinduced effects in the charge-ordering phase with a bicritical behavior competing with ferromagnetic phase have been observed. As shown in Fig. 1, the photoinduced persistent insulator–metal transition in $Pr_{0.55}(Ca_{0.75}Sr_{0.25})_{0.45}MnO_3$ film has been revealed by Takubo *et al.*[44] The transition is caused by the destruction of charge ordering in the immediate neighborhood of the excited sites by photoexcitation. Furthermore, as the reverse phenomenon above, the first persistent photoinduced metal-to-insulator transition has been found as shown in Fig. 2.[45] They considered that the photoexcitation can destabilize the local lattice distortion by creating momentarily a uniform charge distribution and consequently cause the transition.

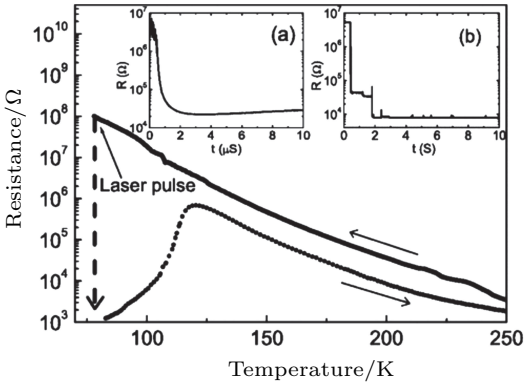


Fig. 1. Temperature dependence of the resistance. Solid and dotted lines denote the cooling and warming processes, respectively. Insets show the resistance drop at individual pulses for various time scales.[44]

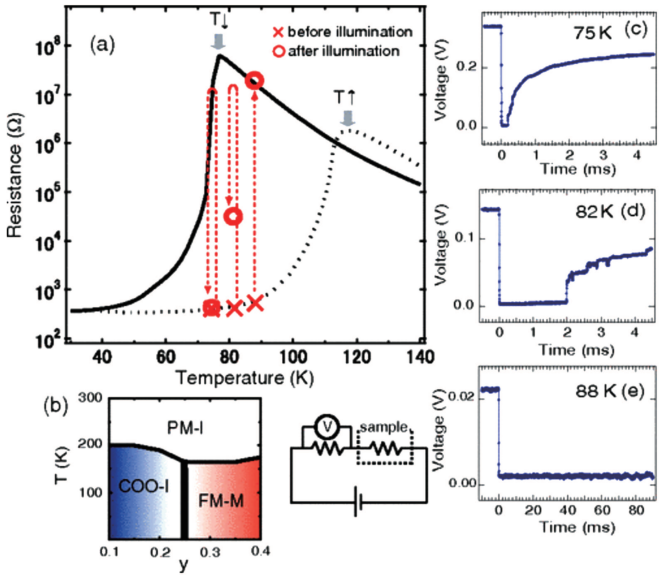


Fig. 2. (color online) (a) Temperature dependence of the resistance. Solid and dotted lines denote the cooling and warming processes, respectively. (b) Phase diagram of $Pr_{0.55}(Ca_{0.75}Sr_{0.25})_{0.45}MnO_3$ film. (c)–(e) Voltage change across the reference resistance caused by the laser illumination.[45]

Moreover, the photoinduced relaxation of resistance can be measured by the experimental setup shown in Fig. 3, which is composed of the triggering timing system and the resistance recording system.[46–48] As shown in Fig. 4, the resistance nonlinearly decreases with the irradiation time when the laser is on and then the resistance restores the original value after irradiation. The experimental data are fitted using the formula

$$R(t) = R_0 + A\exp[-(t/\tau)], \tag{1}$$

where $R(t)$ is the resistance at the irradiation time t and τ is the time constant. The obtained time constant is the characterization of the photoinduced relaxation process, indicating the speed of the relaxation process, which is the process of delocalization.

In addition, the persistent and transient photoinduced effects have been observed in manganites, which originate from different mechanisms, such as the oxygen deficiency in most metallic states and the melting of charge-ordering (CO) state.[49–51] The persistent photoinduced ratio is defined as PPC $= (R_0 - R_b) \times 100\%/R_0$, where R_0 and R_b are the initial resistance without the light illumination and the balanced resistance after the light illumination, respectively. Figure 5 shows the PPC effect for the phase-separated $Sm_{0.5}Sr_{0.5}Mn_{1-y}Cr_yO_3$ ($0 \leq y \leq 0.2$) films under the light illumination as a function of the doping contents and temperatures.[52] We observe an evolution of persistent and transient photoinduced effects induced by impurity doping effects and temperatures, which is closely related with the number of ferromagnetic clusters and paves a way for practical applications in photoelectric devices of all-oxides.

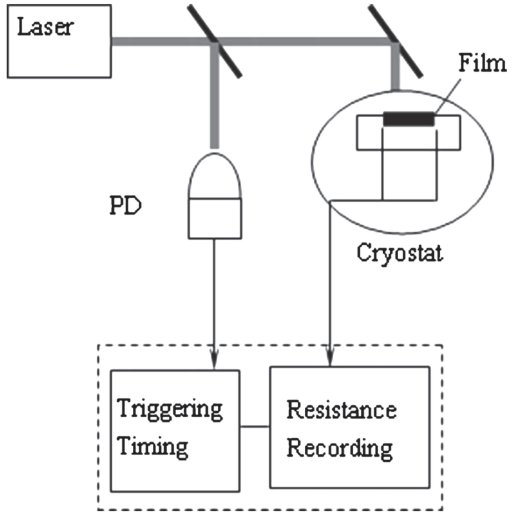


Fig. 3. A schematic view of the photoinduced relaxation character experimental facility. PD is a photodiode.[46]

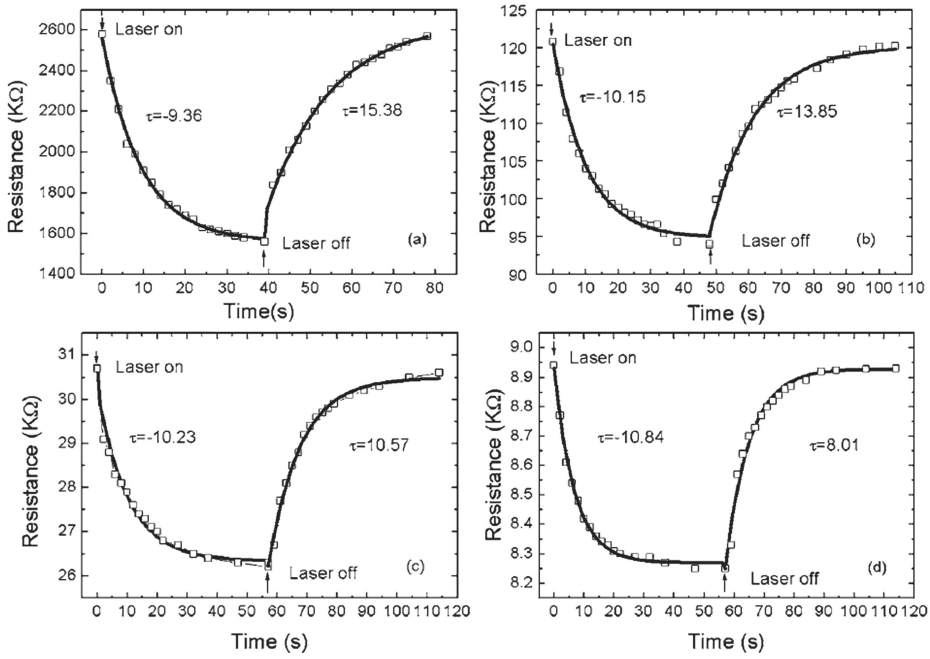


Fig. 4. Photoinduced relaxation characters of the $La_{0.5}Ca_{0.5}MnO_3$ films at different temperatures: (a) 80 K, (b) 140 K, (c) 180 K, (d) 230 K.[46]

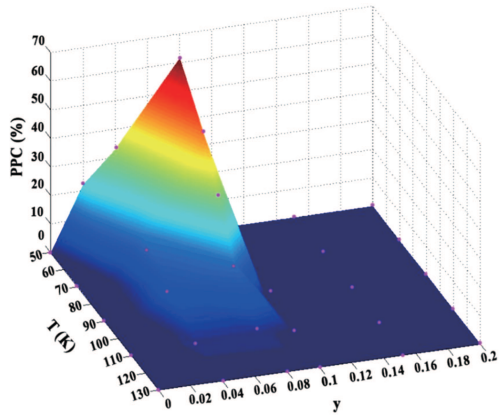


Fig. 5. (color online) PPC effect for the films under the light illumination as a function of the doping contents and temperatures.[52]

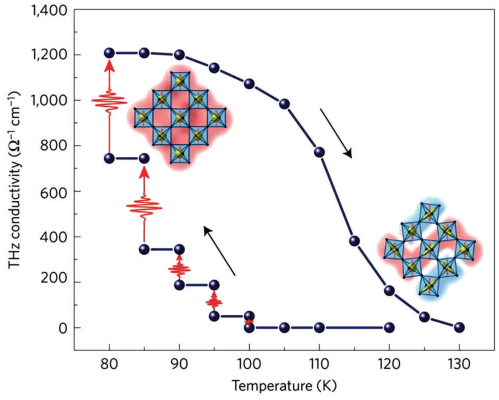


Fig. 6. (color online) Photoinduced insulator to metal phase transition in strain-engineered thin film.[60]

2.2. Manganite systems with the typical metal–insulator transition

For the manganite systems with the typical metal–insulator transition, the photo-irradiation results in an increase of the resistivity of the film in the metallic state and a decrease in the insulating state.[53–58] Generally, the light can excite the downspin e_g electrons, which will destroy the ferromagnetic coupling between the upward-spin e_g and t_{2g} electrons in Mn^{3+} ions. As a result, it weakens the double exchange effect and increases the resistivity. Namely, this is the so-called photoinduced demagnetization. Moreover, according to the double-exchange effect, the probability of the e_g electron transferring from Mn^{3+} to the neighboring Mn^{4+} is proportional to $\cos(\theta/2)$ (θ being the angle between the neighboring spins). Supposing that the interaction of the photo-irradiation causes a change δ of angle θ, the relative change in probability is defined as follows:

$$[\cos(\theta/2+\delta/2)-\cos(\theta/2)]\cos(\theta/2). \tag{2}$$

One obtains the simplified result from Eq. (2)

$$-[1-\cos(\delta/2)+\tan(\theta/2)\sin(\delta/2)], \tag{3}$$

where $\delta/2$ and $\theta/2$ vary from 0 to $\pi/2$. The relative change in Eq. (3) is negative, indicating that the double exchange effect becomes weaker. According to Eq. (3), if the change δ is a fixed constant, the larger value of θ, the larger relative change. Therefore, the relative change in the resistance becomes larger. In the experiments, the condition of each irradiation is identical, accordingly the change δ is a certain value. This model can be used to explain the relation between the relative change in the resistance and the temperature or the strain. Meanwhile, the photoinduced resistance can be erased by a magnetic field.[59] Furthermore, the photoinduced insulator-to-metal phase transition has been observed in strain-engineered $La_{2/3}Ca_{1/3}MnO_3$ film, as shown in Fig. 6.[60] As temperature decreases, photoexcitation yields a step-like conductivity progression until it reaches the hidden metallic state at 80 K. With increasing temperature (without the photoexcitation), the conductivity returns to the insulating phase at 130 K. Recently, some scientists also discovered many emergent physical phenomena and properties. For examples, Li *et al.*[61] successfully fabricated a novel spin transistor with an optical gate by partially illuminating the Hall channel with the blue light of a light-emitting diode (LED). And the study found that this optical gating effect is significantly enhanced with the increase of the optical power and shows repeatable cycling characteristics. Their team also focused on the optical control of the magnetic properties of $La_{1/2}Sr_{1/2}MnO_{3-\delta}$. They manipulated the anisotropic magnetoresistance under the illumination of a common red LED and the window of the anisotropic magnetoresistance curve under the scanning magnetic field is enlarged under red light, indicating an increase in saturation magnetization. The experimental results also showed that the optical control of magnetization is reversible and strongly depends on the light intensity and Mn^{4+} content of $La_{1/2}Sr_{1/2}MnO_{3-\delta}$.[62] Sun *et al.*[63] found that in the bilayered perovskite manganite $La_{2-2x}Sr_{1+2x}Mn_2O_7$ ($x=0.5$ and 0.6), laser irradiation can lead to persistent modifications of both resistance and microstructure in the phase-separated (PS) states. *In situ* laser irradiation can modify the PS nature and strengthen the charge-ordering state. Yada *et al.*[64] performed double-pulse pump experiments in $Pr_{0.6}Ca_{0.4}MnO_3$. The results showed that compared with the single-pulse pump, the photoinduced melting of charge-ordering is enhanced by $\sim 60\%$ by the double-pulse pump. This also indicated that the decrease in crystal anisotropy is a key factor in enhancing the efficiency of photoinduced CO melting. Elovaara *et al.*[65] reported that the laser-irradiated $Pr_{1-x}Ca_xMnO_3$ ($x=0.4$) film achieved a nearly nine orders of magnitude magnetoresistive insulator-to-metal switching of the film in a significantly reduced magnetic field compared to darkness. And this combined effect of light and magnetic field is called magneto-optical resistance (MPR). Yue *et al.*[66] studied a large photo-induced enhanced MR in $La_{2/3}Ca_{1/3}MnO_3$ films on n-Si substrates. The film was irradiated with a 808 nm CW laser in a magnetic field of 6.4 kOe, the MR ratio was sharply increased from 0.54% to 18%. Wang *et al.*[67] reported an ultrafast optical pump-probe measurement with linearly and circularly polarized laser pulses in the manganite $La_{0.67}Ca_{0.33}MnO_3$ thin film and detected the basic process of light–matter interaction in the $La_{0.67}Ca_{0.33}MnO_3$ film induced by femtosecond laser excitation. Esposito *et al.*[68] comprehensively analyzed the photoinduced transition of magnetoresistive manganites. They used femtosecond x-ray diffraction to study the structural response of charge and orbitally ordered $Pr_{1-x}Ca_xMnO_3$ films across a phase transition induced by 800 nm laser pulses. These provide new ideas and directions for further study of manganites, especially about the interaction between light and matter.

3. Photoinduced effect in manganite-based heterostructures

Heterostructure is an important platform for tuning the properties and producing novel effect as well as applications by interface effect and strain engineering.[69–71] As Kroemer, Nobel Prize laureate in physics, said, "Interface is the device".[72] In particular, different substrates and interfaces manipulate the structural symmetry, lattice constant, dimensions, and quantum size of the thin film. Therefore, the energy band structure of manganite is tailored. In this way, the

electronic energy band structure of the film can also be affected due to the limited freedom of movement of the electrons and the interface electronic states generated by the interface interaction coupling. The interface strain is mainly caused by different single crystal substrates. Until now, some materials, such as ZnO, Si, BFO, titanate-based oxides, and $0.7Pb(Mg_{1/3}Nb_{2/3})O_3$-$0.3PbTiO_3$ (PMN-PT) have been integrated with manganites. The overviews are as followed.

3.1. Manganites/ZnO heterostructures

ZnO is an important wide band gap semiconductor with a bandwidth of 3.37 eV. In general, it favors the n-type conduction and possesses a large exciton binding energy. The divalent alkaline-doped manganites exhibit p-type conduction. Thus, the heterostructures combining manganites with n-type ZnO will create novel physical properties. Until now, there are many studies on manganites/ZnO heterostructures, involving electrical characteristics, positive magnetoresistance, and charge-transport mechanism, etc.[73–80] $La_{0.7}Sr_{0.3}MnO_3$ (LSMO) and ZnO layers on $LaAlO_3$ (100) substrates have been fabricated by using a pulsed laser deposition method.[81,82] The schematic illustration and the current–voltage characteristics of the heterostructure at different temperatures are shown in Fig. 7. The positive bias is defined by the current flowing from LSMO to ZnO. The good rectifying behavior of the p–n diodes is observed, which is similar to that of conventional p–n junctions. The diffusion potential V_D is changed from 0.4 V at 277 K to 0.6 V at 77 K and the slope of the I–V curves becomes steeper in the forward mode as the temperature increases. It is known that the carriers can be driven over the energy barrier at the ZnO/LSMO interface by smaller applied voltage as the temperature is increased. Therefore, V_D decreases and the leakage current increases with increasing temperature; consequently, the slope coefficient becomes larger. Furthermore, the photovoltaic voltages with a 248 nm laser irradiation at the energy density of 0.3 mJ/mm^2 as a function of time at 138 K, 238 K, and 358 K are shown in Fig. 8. It is noted that the rise time is about 10 ns. The peak photovoltaic voltages and the full width at half maxima (FWHM) of the heterostructure irradiated by the laser as a function of temperature are shown in the inset. The peak photovoltaic voltages and the FWHM nonlinearly decrease with increasing temperature. It is known that only the photogenerated carriers, located at or reaching the depletion region by diffusion, directly contribute to the photovoltage. As the temperature increases, more carriers pass through the barrier and thereby the accumulated electrons and holes decrease, which results in the decrease in the photovoltages.

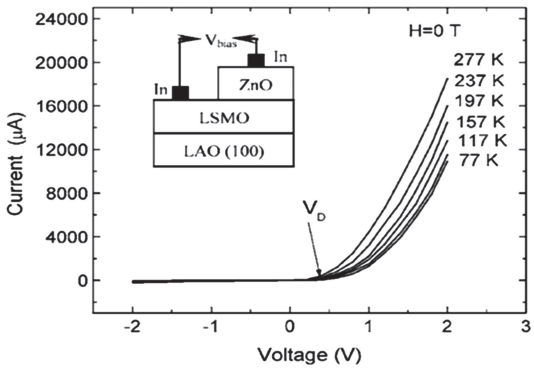


Fig. 7. The I–V characteristics of the heterostructure at different temperatures.[81]

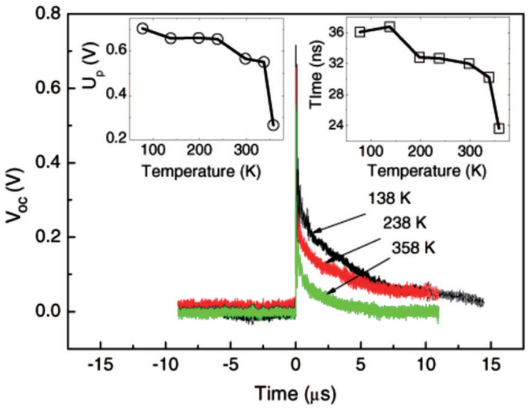


Fig. 8. (color online) Photovoltaic voltage as a function of time at 138 K, 238 K, and 358 K.[82]

3.2. Manganites/Si heterostructures

As an important semiconductor, Si is an indispensable element of modern information industry. Considering the practical applications in devices, it is of special significance to study the integration of manganites with Si. So far, a large amount of phenomena based on manganites/Si heterostructures have been observed, such as photovoltaic effect,[83–87] rectification characteristics,[88] and magnetoresistance.[89–91] For example, Chen *et al.*[92] prepared a $La_{0.88}Te_{0.12}MnO_3$/Si heterostructure using a pulsed laser deposition method. The heterostructure has a photovoltaic effect and good rectification. Xing *et al.*[93] investigated the side-illumination-induced enhancement of photovoltaic response in $La_{0.9}Sr_{0.1}MnO_3$/Si heterostructures. The photovoltaic responsivity can reach 6.87 mV·mW^{-1} under the side illumination, which is much larger than 0.17 mV·mW^{-1} under the normal illumination.

We have deposited the $La_{0.7}Sr_{0.3}MnO_3$ (LSMO) film on a single-crystal Si (100) substrate.[94] The temperature dependence of the resistivity is shown in the inset of Fig. 9, in which the LSMO film exhibits the typical metal–insulator transition at $T = 143$ K. It is interesting to note that a local minimum of photovoltage also seems to occur at $T = 143$ K, which is consistent with the transition temperature. This indicates that the phase transition of the LSMO film affects the photovoltaic effect. The photovoltages are usually related to the accumulation of the photogenerated carriers and the width of the depletion layer. When the temperature is increased, the accumulation of the photogenerated carriers is reduced because of the stronger

thermal fluctuation, resulting in a decrease of the photovoltages. At $T = 143$ K, the LSMO film undergoes a change in the band structure accompanying a metal–insulator transition, i.e., the up-spin and down-spin subbands split. The spin-polarized carriers tend to occupy the lower subbands, which may cause the thinner thickness of the depletion layer at the heterostructure. Thus, this will result in an appearance of the local minimum of the photovoltages at $T = 143$ K.

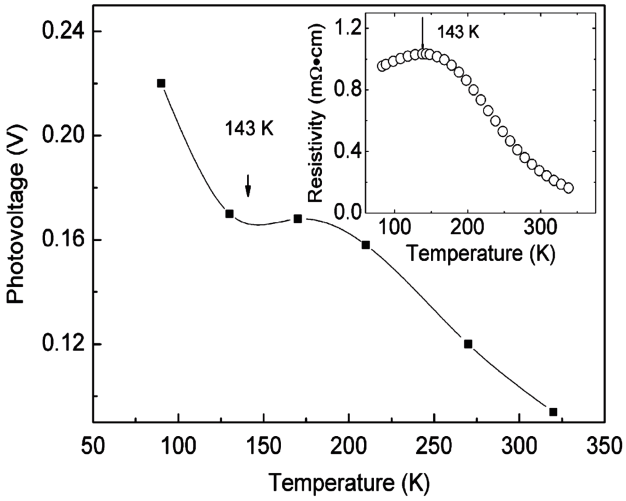


Fig. 9. Temperature dependence of the maximum photovoltages. Inset shows the temperature dependence of resistivity of the LSMO film.[94]

In addition, we also investigated the photoinduced effect on carrier transport properties in the LSMO/Si heterostructures.[95] Figure 10 shows the temperature dependence of the resistance and the relative change of the photoinduced resistance in the current-perpendicular-to-plane (CPP) geometry. The heterostructure without laser irradiation has a metal–insulator transition at $T = 270$ K. And the heterostructure in the CPP geometry exhibits a transient photoconductivity effect. The maximum relative change of photoinduced resistance in LSMO/Si heterostructures at a temperature of 270 K is approximately 6200%, and the relative change can reach 5674% at room temperature. The giant change in resistance is attributed to laser-created carriers in the heterostructure. As we know, the band gaps of LSMO and Si are 1.0–1.3 eV and 1.12 eV, respectively.[96] The photon energy of the laser (about 2.34 eV) in the experiments is larger than their band gaps. Under laser irradiation, the created electrons and holes in LSMO and Si move to the Si and LSMO sides, respectively. Therefore a drastic reduction in resistance (by more than three orders of magnitude) occurs. The resistance of the heterostructure irradiated by laser as a function of the power level at 100 K and 240 K is shown in the inset, which clearly shows a nonlinear behavior. This relation is described by a simple power law $R \propto P^{-n}$, where R is the resistance and P is the power level of the laser. The solid lines are the fitting curves in the inset of Fig. 10, from which we obtain that the exponent n is about 0.13 at $T = 100$ K and 240 K. This indicates that the recombination rate is exponentially proportional to the concentration of laser created carriers.

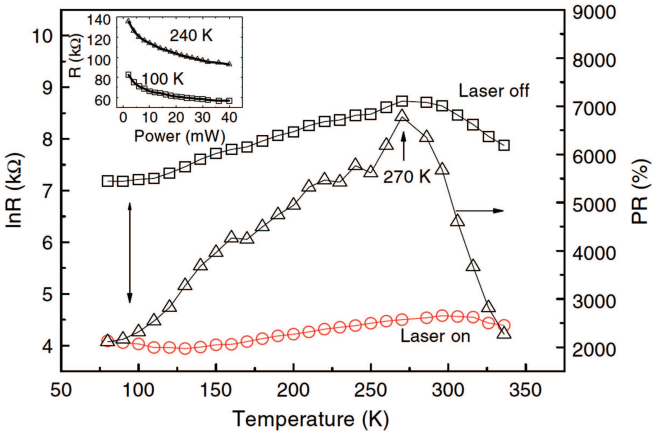


Fig. 10. (color online) Temperature dependence of resistance and PR of the heterostructure in CPP geometry. The resistance is given on a natural log scale. The resistance as a function of power level at 100 K and 240 K is shown in the inset and the solid lines are the fitted curves using a simple power law.[95]

3.3. Manganites/BFO heterostructures

As early as 2003, the multiferroic properties of single-phase BFO were observed.[97] Then, researches on perovskite single-phase multiferroic materials attracted much attention again.[98,99] In particular, the BFO has excellent photoelectric properties.[100–104] Nevertheless, the magnetism of BFO is very weak and thus researchers want to enhance it through compositing with other materials. We have prepared BFO/$La_{1/3}Sr_{2/3}MnO_3$ heterostructures.[105] The results show that BFO/ $La_{1/3}Sr_{2/3}MnO_3$ heterostructures retain multiferroic properties and furthermore magnetic properties are enhanced because of the interfacial effect. In addition, the photovoltaic effect was also observed in the heterostructures.[106,107] It is observed that the short-circuit current is inverted with the change of polarization of the BFO layer. Figure 11(a) shows the time dependence of the short-circuit photocurrent at an incident laser density of 91.4 mW/cm^2 and zero bias. We can see that the photocurrent increases suddenly to a transient maximum and then reaches a steady state. When the BFO is poled along the two opposite directions, the photocurrent and photovoltage are switched (see Fig. 11(b)), indicating that the ferroelectric polarization has a dominant role in the photovoltaic effect. On the other hand, asymmetric properties between the negatively poled film and the positively poled film are observed, which may be caused by the contribution from the electrode/film interface. Therefore, the photovoltaic effect in the heterostructure is due to the contribution from both the ferroelectric polarization and the electrode/film interface. Figure 12 shows the I–V curves taken in the dark, under 160 mW/cm^2 and 200 mW/cm^2 green-light illumination ($\lambda = 532$ nm), suggesting that photoconductivities increase

with enhancing light intensity. The resulting current of photoexcited carriers, driven by the intrinsic polarization, can be described by the following equation:[108]

$$J = \left(\sigma_{\rm d} + \sigma_{\rm ph}\right)\xi, \tag{4}$$

where $\sigma_{\rm d}$ and $\sigma_{\rm ph}$ represent the dark and light components of the conductivity, respectively. In principle, thermal variation induced by visible-light illumination can contribute to the photoconductivity, but the decrease of the resistance due to a light-induced temperature increasing causes a less negative photoconductivity increasing. These findings are consistent with the model present in Eq. (4) and serve as an evidence of the photoconductivity effect in BFO.

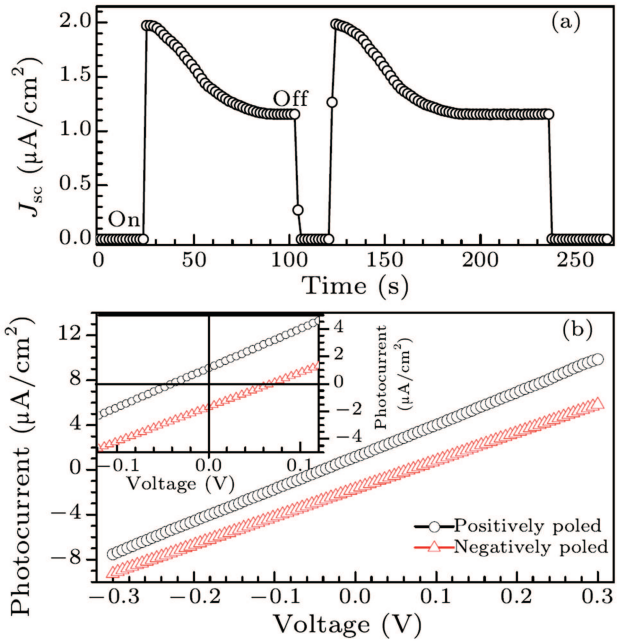


Fig. 11. (color online) (a) The time dependence of the photo current under zero bias and an incident laser intensity of 91.4 mW/cm^2, (b) J–V curves measured with laser incident.[106]

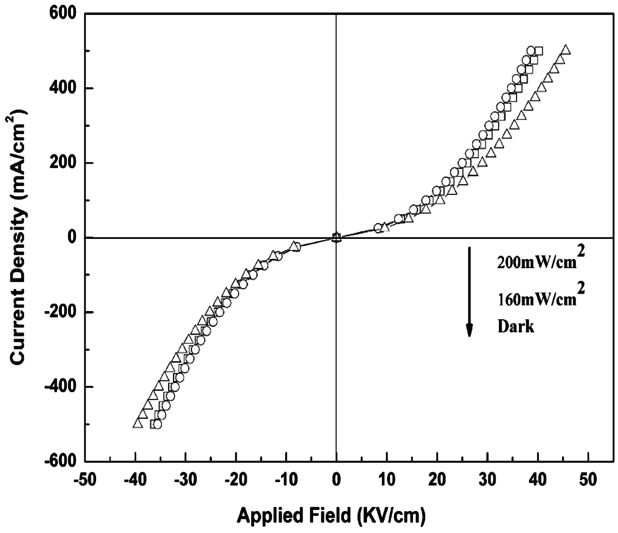


Fig. 12. Dark, 160 mW/cm^2, and 200 mW/cm^2 green-light current density as a function of applied field for the heterostructure.[107]

3.4. Manganites/titanate-based oxides heterostructures

Titanate-based oxide, a perovskite material with a high dielectric constant, has potential applications for dynamic random access memory (DRAM) devices, and its dielectric constant can also be adjusted by an external field. At the same time, manganites-based heterostructures have also attracted wide attention with the gradual deepening study of different functional devices with different structures.[109–114] Recently, many researchers have conducted in-depth studies on the photoelectric effect of heterostructures, such as manganite/Nb:$SrTiO_3$ heterostructures.[115–118] We prepared phase-separated manganite heterostructures $(Pr_{0.65}(Ca_{0.75}Sr_{0.25})_{0.35}MnO_3$ (PCSMO)/Nb:$SrTiO_3$ by the pulsed laser deposition. The optoelectronic properties of the heterostructures under the application of a magnetic field were investigated. As shown in Fig. 13, it is found that the relative change in photovoltaic (PV) values at 140 K reaches 63% under 1 T magnetic field, indicating that the magnetic field is an important factor affecting the photovoltaic effect.[119] At the same time, a monovalent Ag-doped manganite $La_{0.8}Ag_{0.2}MnO_3$ (LAMO)/Nb: $SrTiO_3$ heterostructure has also been prepared and exhibits good rectification characteristics.[120] The photovoltage and light intensity satisfy the classical exponential relationship with the increase of the light intensity, as shown in Fig. 14. Apparently, the photovoltage grows with the increase in power, and tends to saturate (~ 0.76 V) once the power reaches 0.3 W. When the light power increases, more electron–hole pairs are excited, which results in an increase in $V_{\rm oc}$. However, the photovoltage is limited by the original barrier height, and the maximum $V_{\rm oc}$ is close to the diffusion voltage. In the power range of -0.3 W, the data analysis shows very poor agreement with the exponential relationship. However, the fitting in the range 0–0.1 W shows good agreement. This indicates that the idealized p–n diode can partly describe the photovoltaic effect of the LAMO/ Nb:$SrTiO_3$ heterojunction. Furthermore, the rectifying characteristics and photovoltaic effect of $TbMnO_3$ (TMO)/Nb:$SrTiO_3$ heterostructures were studied systematically. Figure 15 shows the relationship between the photovoltage and time in the heterostructure irradiated by a 248 nm light at the temperature of 300 K. The maximum photovoltage is about 0.119 V at 0.71 mJ/mm^2. That work provides the possibility for TMO applications in ultraviolet (UV) light.[121] In addition, Sheng *et al.* deposited 24 nm LSMO thin films on the (001) and (110) crystal planes of $SrTiO_3$-Nb. From Fig. 16, it can be seen that the correlation gap E_g plays a decisive role in the amplitude $J_{\rm ph}$, its temperature and magnetic adjustability of heterostructures.[122]

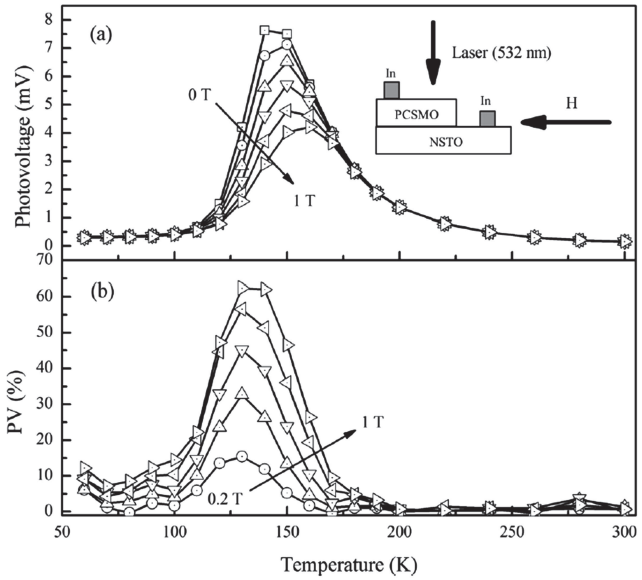


Fig. 13. Temperature dependence of (a) photovoltage of heterostructure irradiated by a laser, (b) PV for PCSMO/ Nb:$SrTiO_3$ under different magnetic fields, respectively. Inset: the schematic diagram of heterostructure under magnetic field and light.[119]

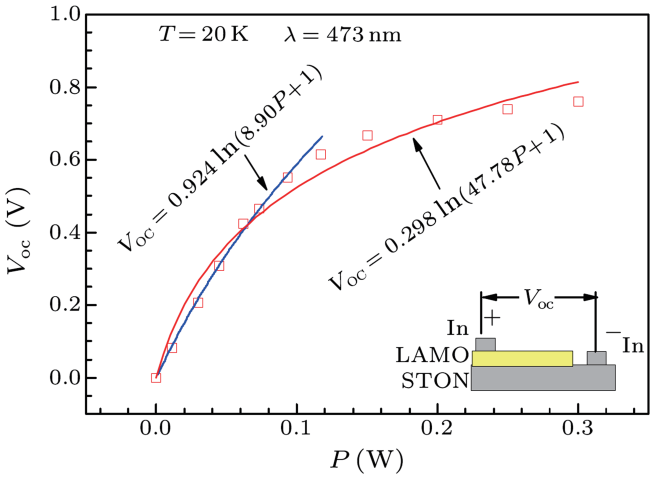


Fig. 14. (color online) Photovoltage versus power under the illumination of a 473 nm laser beam at 20 K. Inset is the structure of the film.[120]

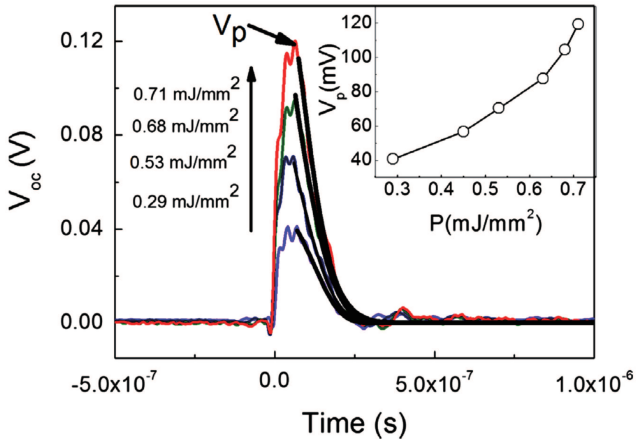


Fig. 15. (color online) Photovoltages of the heterostructure under the irradiation of a laser (248 nm) at $T = 300$ K as a function of time. The inset shows the peak photovoltages as a function of the power density.[121]

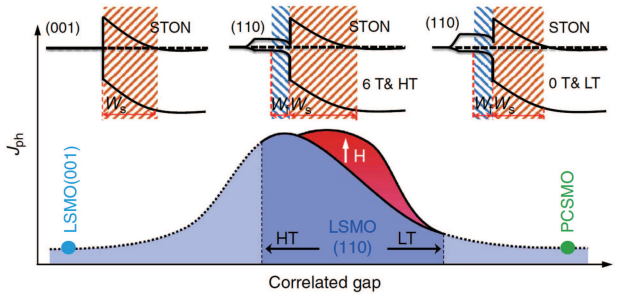


Fig. 16. (color online) A schematic image of the relationship between J_{SC} and correlated gap in correlated junctions. The insets show the schematic band diagrams for (left) LSMO (001) junctions, (middle) LSMO (110) junction under high magnetic field (6 T) or high temperature (HT), and (right) LSMO (110) junction without magnetic field (0 T) or low temperature (LT), respectively.[122]

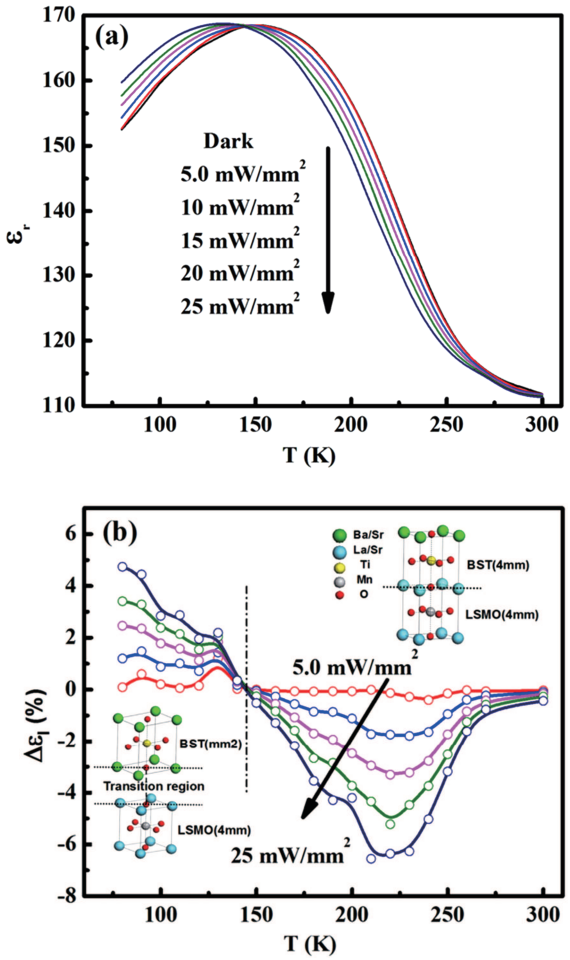


Fig. 17. (color online) Dielectric constant (a) and its relative variation (b) as a function of temperature for the BST/$La_{0.67}Sr_{0.33}MnO_3$ heterostructure exposed to light of different intensities with an interval of 5 mW/mm^2. Inset: the sketches of the crystal lattice structure for the $La_{0.67}Sr_{0.33}MnO_3$ and barium titanate layers at different temperature ranges.[123]

Besides, we systematically studied the microstructure, leakage current, and tunability of the dielectric constant of the barium titanate/manganite heterostructures induced by an optical field. As shown in Fig. 17, it is worth noted that the relative change in the dielectric constant has a positive to negative transition at 150 K when the heterostructure is

irradiated by a light.[123] In the experiment, the photon energy of about 2.34 eV (532 nm) is smaller than the band gap of $Ba_{0.6}Sr_{0.4}TiO_3$ (BST) ($\sim$ 3.0 eV) and larger than that of $La_{0.67}Sr_{0.33}MnO_3$. Moreover, the transmission of the Pt film (electrode material) is about 36% at 532 nm. Accordingly, the light can generate the carriers in the $La_{0.67}Sr_{0.33}MnO_3$ layer by passing through the BST layer and Pt film when the heterostructure is irradiated. And the photoinduced carriers at the BST/$La_{0.67}Sr_{0.33}MnO_3$ interface change the interfacial polarization and thus affect the dielectric properties.[124] These results may be useful in developing potential applications of heterojunctions for optoelectronic detections.[125–131]

3.5. Manganites/PMN-PT heterostructures

The combination of a manganite thin film and a ferroelectric PMN-PT single crystal is a promising platform. It is considered as a convenient method to modulate the physical properties of films.[132–137] An electric field can be applied to the substrate and thus the lattice constant of PMN-PT can be continuously adjusted by utilizing the electrostriction effect. So, the physical properties of the film can be continuously controlled.[138–142] If an ultra-thin film is grown, the interface polarization of PMN-PT will play a dominant role. It can also be considered as a ferroelectric field effect transistor, in which manganite and PMN-PT substrates serve as conductive path and insulated gate, respectively. The electric field-induced polarization of the ferroelectric layer can not only generate the lattice distortion, but also generate charge accumulation or depletion at the interface.

Here, a $Pr_{0.65}(Ca_{0.75}Sr_{0.25})_{0.35}MnO_3$ (PCSMO) thin film was deposited on the piezoelectric PMN-PT substrate by pulsed laser deposition. Besides the observed persistent magnetoresistance effect,[143] the PCSMO/PMN-PT heterostructure exhibits a reversible bistability in the photoinduced change in resistance at $T < 80$ K as the voltages are increased.[144] We define the photoinduced change in the resistance (PR), $\mathrm{PR} = \left(R_{\mathrm{dark}} - R_{\mathrm{light}}\right)/R_{\mathrm{dark}} \times 100\%$. As shown in Fig. 18(a), the film exhibits the transient photoinduced effect (TPE) and the PR is reduced under the applied voltage, demonstrating that the applied voltage seems to impose an active suppression on the TPE. The TPE becomes more complex with the decrease of temperature. It should be noted that the values of normalized PR undergo a significant crossover from positive to negative when the applied voltages increase up to a critical value. It indicates that the electric field modulates the TPE and induces an appearance of the bisable states. Meanwhile, the transition voltages are increased with increasing temperature. In other words, the bistable state of PR requires the larger voltage at the higher temperatures. The electric field modulation of bistability in the PCSMO/PMN-PT heterostructure provides us with some deep insights into understanding the physical mechanisms of coupling effects of external fields in electric phase separation manganites.

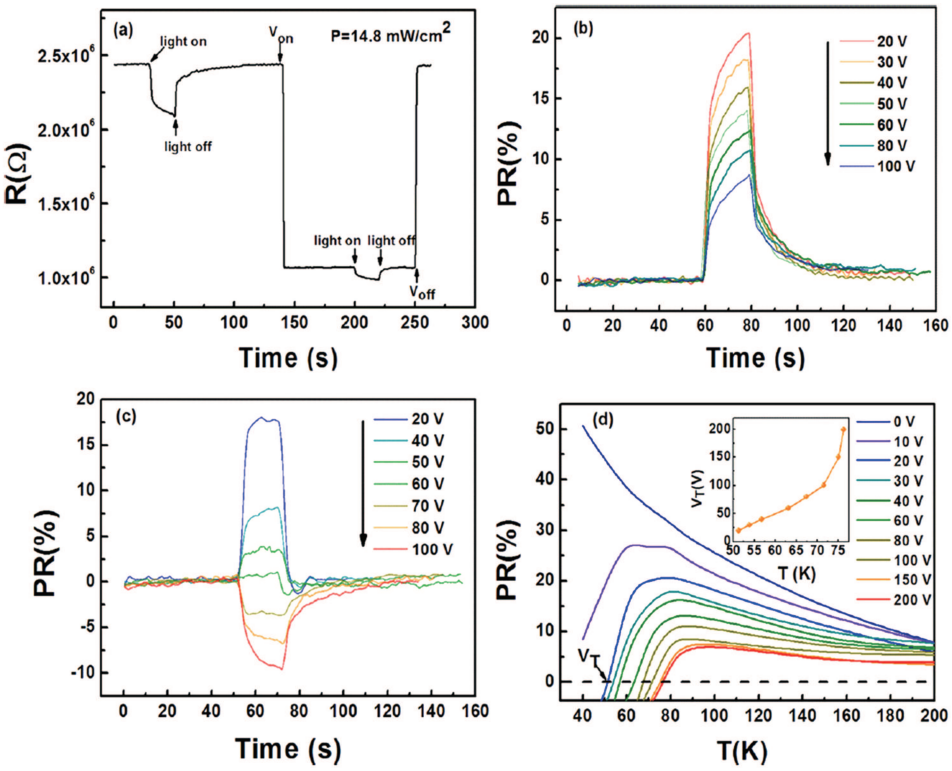


Fig. 18. (color online) (a) Resistance as a function of elapsed time upon the application of light irradiation and bias voltage 40 V at 150 K. (b) and (c) Variation of normalized PR under the different voltages at 65 K and 80 K, respectively. (d) Temperature dependence of PR for the PCSMO film by applying different bias voltages. The inset shows the temperature dependence of V_T.[144]

4. Conclusion and perspectives

In summary, the transition metal oxide systems with perovskite structures are a veritable storehouse of abundant physical properties. Manganites are one drop in the ocean and there are many original properties that need to be explored and excavated. On the one hand, researching on the manganites and their heterostructures photoinduced effects provide us opportunities to understand the physical mechanisms of manganites, multiphase coexistence, magnetoelectric coupling, and other rich effects deeply. On the other hand, in terms of the exploration and development of dynamic random access memory and optoelectronic devices, this review also provides us with some insights and theoretical support. In addition, as a powerful method, the photoinduced effect can also be extended to other related systems and may produce novel performance and effect. This brief review just likes a glimpse in the pipe, providing simple investigations of photoinduced effect in manganites and their heterostructures. There are still a lot of issues that need to be solved. Future research will focus on the study of intrinsic mechanisms of the non-equilibrium physics at the quantum scale and interface, especially about the multifunctional and multi-field coupling with strong correlations, which may be useful in developing responsive and memorized devices of external fields.

References

[1] Fausti D, Tobey R I, Dean N, Kaiser S, Dienst A, Hoffmann M C, Pyon S, Takayama T, Takagi H and Cavalleri A 2011 *Science* **331** 189
[2] Mankowsky R, Subedi A, Först M, Mariager S O, Chollet M, Lemke H T, Robinson J S, Glownia J M, Minitti M P, Frano A, Fechner M, Spaldin N A, Loew T, Keimer B, Georges A and Cavalleri A 2014 *Nature* **516** 71
[3] Fiebig M, Lottermoser T, Meier D and Trassin M 2016 *Nat. Rev. Mater.* **1** 16046
[4] Duan C G 2009 *Prog. Phys.* **29** 215
[5] Zhou Y C, Fang D N and Zhen X J 2009 *Bull. Natl. Nat. Sci. Found. Chin.* **2** 78
[6] Shi Z, Wang C P and Liu X J 2008 *Chin. Sci. Bull.* **53** 2135
[7] Jin S, Tiefel T H, McCormack M, Fashtnacht R A, Ramesh R and Chen L H 1994 *Science* **264** 413
[8] Hwang Y, Iwasa Y, Kawasaki M, Keimer B, Nagaosa N and Tokura Y 2012 *Nat. Mater.* **11** 10
[9] Yan H, Zhang Z T, Wang S H, Wei X Y, Chen C L and Jin K X 2018 *Acs Appl. Mater. Interfaces* **10** 14209
[10] Ohtomo A and Hwang H Y 2004 *Nature* **427** 423
[11] Jin K X, Lin W, Luo B C and Wu T 2015 *Sci. Rep.* **5** 8778
[12] Yan H, Zhang Z T, Wang S H, Zhang H R, Chen C L and Jin K X 2017 *Acs Appl. Mater. Interfaces* **9** 39011
[13] Helmholt R, Wecker J, Holzapfel B, Schultz L and Samwer K 1993 *Phys. Rev. Lett.* **71** 2331
[14] Zener C 1951 *Phys. Rev.* **82** 403
[15] Millis A J, Littlewood P B and Shraiman B I 1996 *Phys. Rev. Lett.* **77** 175
[16] Dagotto E, Hotta T and Moreo A 2001 *Phys. Rep.* **344** 1
[17] Ding J F, Jin K X and Zhang Z 2012 *Appl. Phys. Lett.* **100** 062402
[18] Jin K X, Zhao S G and Chen C L 2008 *Mater. Lett.* **62** 1061
[19] Miyano T, Tanaka Y, Tomioka and Tokura Y 2005 *Phys. Rev. Lett.* **95** 017404
[20] Kiryukhin V, Casa D, Hill J P, Keimer B, Vigliante A, Tomioka Y and Tokura Y 1997 *Nature* **386** 813
[21] Raveau B, Maignan A and Martin C J 1997 *Solid State Chem.* **130** 162
[22] Asamitsu A, Tomioka Y, Kuwahara H and Tokura Y 1997 *Nature* **388** 50
[23] Jin K X, Chen C L, Zhao S G and Song Z M 2006 *J. Mater. Sci.* **41** 3881
[24] Asamitsu A, Tomioka Y, Kuwahara H and Tokura Y 1997 *Nature* **388** 50
[25] Polli D, Rini M, Wall S, Schoenlein R W, Tomioka Y, Tokura Y, Cerullo G and Cavalleri A 2007 *Nat. Mater.* **6** 643
[26] Ichikawa H, Nozawa S, Sato T, Tomita A, Ichiyanagi K, Chollet M, Guerin L, Dean N, Cavalleri A and Adachi S 2011 *Nat. Mater.* **10** 101
[27] Dagotto E 2005 *Science* **309** 257
[28] Tokura Y 2006 *Rep. Prog. Phys.* **69** 797
[29] Yi D, Lu N P, Chen X G, Shen S C and Yu P 2017 *J. Phys.: Condens. Matter* **29** 443004
[30] Liao Z L, Huijben M, Koster G and Rijnders G 2017 *Appl. Phys. Rev.* **4** 041103
[31] Prellier W, Lecoeur P and Mercey B 2001 *J. Phys.: Condens. Matter* **13** R915
[32] Haghiri-Gosnet A M and Renard J P 2003 *J. Phys. D: Appl. Phys.* **36** R127
[33] Van T G, Lebedev O, Hervieu M and Raveau B 2004 *Rep. Prog. Phys.* **67** 1315
[34] Wang J, Malik I A, Liang R R, Huang W, Zheng R K and Zhang J X 2015 *Chin. Phys. B* **24** 070304
[35] Zhang T, Wang X P, Fang Q F and Li X G 2014 *Appl. Phys. Rev.* **4** 029901
[36] Liu Y K, Yin Y W and Li X G 2013 *Chin. Phys. B* **22** 087502
[37] Siwach P K, Singh H K and Srivastava O N 2008 *J. Phys.:Condens. Matter* **20** 273201
[38] Liu J M and Wang K F 2005 *Prog. Phys.* **25** 82
[39] Dong S and Liu J M 1967 *Prog. Phys.* **30** 1
[40] Ge C, Jin K J, Lu H B and Wang C 2009 *Mod. Phys. Lett.* **9** 1129
[41] Wang C, Jin K J, Guo H Z, Lu H B, Wang C, He M and Yang G Z 2011 *Prog. Phys.* **31** 137
[42] Matsubara M, Okimoto Y, Ogasawara T, Tomioka Y, Okamoto H and Tokura Y 2007 *Phys. Rev. Lett.* **99** 207401
[43] Satoh T, Kikuchi Y, Miyano K, Pollert E, Hejtmanek J and Jirak Z 2002 *Phys. Rev. B* **65** 125103
[44] Takubo N, Ogimoto Y, Nakamura M, Tamaru H, Lzumi M and Miyano K 2005 *Phys. Rev. Lett.* **95** 017404
[45] Takubo N, Onishi I, Takubo K, Mizokawa T and Miyano K 2008 *Phys. Rev. Lett.* **101** 177403
[46] Zhao S G, Jin K X and Chen C L 2007 *J. Appl. Phys.* **101** 083701
[47] Zhao S G, Jin K X, Luo B C, Wang J Y and Chen C L 2012 *Acta Phys. Sci.* **61** 047501
[48] Jin K X, Zhao S G, Tan X Y, Chen C L and Jia X W 2009 *Mater. Chem. Phys.* **115** 599
[49] Matsubara M, Okimoto Y, Ogasawara T, Iwai S, Tomioka Y, Okamoto H and Tokura Y 2008 *Phys. Rev. B* **77** 094410
[50] Jin K X, Chen C L, Wang S L, Wang Y L, Wang Y C, Song Z M and Ren R 2004 *J. Appl. Phys.* **96** 1537
[51] Beyreuther E, Thiessen A, Grafstrom S, Eng L M, Dekker M C and Doerr K 2009 *Phys. Rev. B* **80** 075106
[52] Chai X J, Xing H and Jin K X 2016 *Sci. Rep.* **6** 23280
[53] Jin K X, Zhao S G, Chen C L, Du L F, Du Y C, Guo Y H and Xing H 2009 *J. Alloys Compd.* **470** 552
[54] Jin K X, Zhao S G, Wang J Y, Chen C L and Tan X Y 2009 *Appl. Phys. A* **95** 789
[55] Jin K X, Chen C L and Zhao S G 2007 *J. Mater. Sci.* **42** 9617
[56] Zhao S G, Jin K X and Chen C L 2007 *Phys. Scr.* **75** 656
[57] Jin K X, Chen C L, Zhao S G and Song Z M 2006 *Mater. Sci. Eng. B* **127** 285
[58] Jin K X, Zhao S G and Chen C L 2009 *Acta Phys. Sci.* **58** 4953
[59] Guo E, Wang J L, Lu H B, Guo H Z, He M, Jin K J, Yang G Z and Gao J 2012 *Appl. Phys. Lett.* **100** 061902
[60] Zhang J D, Tan X L, Liu M K, Teitelbaum S W, Post K W, Jin F, Nelson K A, Basov D N, Wu W B and Averitt R D 2016 *Nat. Mater.* **15** 956
[61] Li F, Song C, Cui B, Peng J, Gu Y, Wang G and Pan F 2017 *Adv. Mater.* **29** 1604052
[62] Li F, Song C, Wang Y Y, Cui B, Mao H J, Peng J J, Li S N and Pan F 2016 *Phys. Rev. B* **93** 024406
[63] Sun K, Sun S S, Li X Y, Li Z W, Zhang R X, Wei L L, Guo C, Zheng D G, Tian H F, Yang H X and Li J Q 2016 *Phys. Rev. B* **94** 205108

[64] Yada H, Ijiri Y, Uemura H, Tomioka Y and Okamoto H 2016 *Phys. Rev. Lett.* **116** 076402
[65] Elovaara T, Majumdar S, Huhtinen H and Paturi P 2015 *Adv. Funct. Mater.* **25** 5030
[66] Yue Z J, Zhao K, Ni H, Zhao S Q, Kong Y C, Wong H K and Wang A J 2011 *J. Phys. D: Appl. Phys.* **44** 095103
[67] Wang H, Jin Z, Liu X, Zhang Z, Cheng Z and Ma G 2017 *Appl. Phys. Lett.* **110** 252407
[68] Esposito V, Rettig L, Abreu E, Bothschafter E M, Ingold G, Kawasaki M, Kubli M, Lantz G, Nakamura M, Rittman J, Savoini M, Tokura Y, Staub U, Johnson S L and Beaud P 2018 *Phys. Rev. B* **97** 014312
[69] Ramesh A R and Keramidas V G 1995 *Annu. Rev. Mater. Res.* **25** 647
[70] Zubko P, Gariglio S, Gabay M, Ghosez P and Triscone J M 2011 *Annu. Rev. Condens. Matt. Phys.* **2** 141
[71] Guo H Z, Lu H, Jin K J, Lu H B, He M, Wang C and Yang G Z 2010 *Physics* **39** 522
[72] Kroemer H 2000 *Nobel Lecture*
[73] Khachar U D, Solanki P S, Choudhary R J, Phase D M, Ganesan V and Kuberkar D G 2012 *Appl. Phys. A* **108** 733
[74] Tiwari A, Jin C, Kumar D and Narayan J 2003 *Appl. Phys. Lett.* **83** 1773
[75] Chattopadhyay S, Panda J and Nath T K 2013 *J. Appl. Phys.* **113** 194501
[76] Zhang J Q, Huang K K, Si W Z, Wu X F, Cheng G and Feng S H 2013 *Sci. Chin. Chem.* **56** 583
[77] Sun Z H, Ning T Y, Zhou Y L, Zhao S Q and Cao L Z 2008 *Chin. Phys. Lett.* **25** 1861
[78] Solanki P S, Khachar U, Vagadia M, Ravalia A, Katba S and Kuberkar D G 2015 *J. Appl. Phys.* **117** 145306
[79] Feng Y C and Zhang M 2010 *J. Magn. Magn. Mater.* **322** 2675
[80] Ma J J, Jin K X, Luo B C, Fan F, Xing H, Zhou C C and Chen C L 2010 *Chin. Phys. Lett.* **27** 107304
[81] Jin K X, Zhao S G, Chen C L, Wang J Y and Luo B C 2008 *Appl. Phys. Lett.* **92** 112512
[82] Jin K X, Zhao S G, Chen C L, Tan X Y and Jia X W 2009 *J. Phys. D: Appl. Phys.* **42** 015001
[83] Liu X B, Jin L B, Lu H B and Gao J 2016 *Appl. Phys. Lett.* **108** 173502
[84] Jin K X, Zhao S G, Wang J Y, Luo B C and Chen C L 2012 *Appl. Phys. A* **106** 219
[85] Yan Z J, Yuan X, Xu Y B, Gao G M, Jin K X and Chen C L 2007 *J. Phys. D: Appl. Phys.* **40** 2797
[86] Zhao K, Jin K J, Lu H B, Huang Y H, Zhou Q L, He M, Chen Z H, Zhou Y L and Yang G Z 2006 *Appl. Phys. Lett.* **88** 141914
[87] Lu H B, Jin K J, Huang Y H, He M, Zhao K, Cheng B L, Chen Z H, Zhou Y L, Dai S Y and Yang G Z 2005 *Appl. Phys. Lett.* **86** 241915
[88] Wan J Y, Jin K X, Chen C L and Tan X Y 2010 *Acta Phys. Sin.* **59** 8137 (in Chinese)
[89] Yang F, Jin K J, Huang Y H, He M, Lv H B and Yang G Z 2010 *Chin. Phys. B* **19** 14
[90] Jin K X, Zhao S G, Tan X Y and Chen C L 2008 *J. Phys. D: Appl. Phys.* **41** 135003
[91] Jin K X, Li H, Wang J Y, Tan X Y, Zhao S G and Chen C L 2012 *Thin Solid Films* **520** 4493
[92] Chen P, Jin K X, Chen C L and Tan X Y 2011 *Acta Phys. Sin.* **60** 067303 (in Chinese)
[93] Xing J, Zhao K, Liu G Z, He M, Jin Juan K and Lu B H 2007 *J. Phys. D: Appl. Phys.* **40** 5892
[94] Jin K X, Zhao S G, Tan X Y and Chen C L 2008 *Mater. Lett.* **62** 4452
[95] Jin K X, Zhao S G, Tan X Y and Chen C L 2008 *J. Phys. D: Appl. Phys.* **41** 045105
[96] Lu H B, Jin K J, Huang Y H, He M, Zhao K, Cheng B L, Chen Z H, Zhou Y L, Dai S Y and Yang G Z 2005 *Appl. Phys. Lett.* **86** 241915
[97] Wang J, Neaton J B, Zheng H, Nagarajan V, Ogale S B, Liu B, Viehl, D, Vaithyanathan V, Schlom D G, Waghmare U V, Spaldin N A, Rabe K M, Wuttig M and Ramesh R 2003 *Science* **299** 1719
[98] Li P, Dong X L, Gao Y Q and Jin K X 2016 *Opt. Express* **24** 9119
[99] Jin K X, Luo B C, Zhao S G, Wang J Y and Chen C L 2011 *Chin. Phys. Lett.* **28** 87301
[100] Li H, Jin K X, Yang S H, Wang J, He M, Luo B C, Wang J Y, Chen C L and Wu T 2012 *J. Appl. Phys.* **112** 83506
[101] Luo B C, Chen C L and Jin K X 2012 *Mater. Chem. Phys.* **132** 364
[102] Fan F, Luo B, Duan M M, Xing H, Jin K X, Chen C L 2012 *Appl. Surf. Sci.* **258** 7412
[103] Luo B C, Chen C L and Jin K X 2011 *Solid. State. Commun.* **151** 712
[104] Luo B C, Zhou C C, Chen C L and Jin K X 2009 *Acta Phys. Sin.* **58** 4563 (in Chinese)
[105] Zhou C C, Luo B C, Jin K X, Cao X S and Chen C L 2010 *Solid State Commun.* **150** 1334
[106] Luo B C, Chen C L, Fan F and Jin K X 2012 *Chin. Phys. Lett.* **29** 018104
[107] Zhou C C, Jin K X, Luo B C, Cao X S and Chen C L 2010 *Mater. Lett.* **64** 1713
[108] Basu S R, Martin L W, Chu Y H, Gajek M, Ramesh R, Rai R C, Xu X and Musfeldt J L 2008 *Appl. Phys. Lett.* **92** 091905
[109] Jin K X, Luo B C, Li Y F, Chen C L and Wu T 2013 *J. Appl. Phys.* **114** 033509
[110] Du Y M, Peng H Y, Mao H Y, Jin K X, Wang H, Li F, Gao X Y, Chen W and Wu T 2015 *ACS Appl. Mater. Interfaces* **7** 11309
[111] Wang J Q, Barker R C, Cui G J, Tamagawa T and Halpern B L 1997 *Appl. Phys. Lett.* **71** 3418
[112] Wang C, Liu Z L, Liu J M, Chen X M, Cui H Y, Xia C S, Yang Y and Lu W 2008 *Acta Phys. Sin.* **57** 502 (in Chinese)
[113] Yang F, Jin K J, Huang Y H, He M, Lu H B and Yang G Z 2010 *Chin. Phys. B* **19** 087301
[114] Katsu H, Tanaka H and Kawai T 2000 *Appl. Phys. Lett.* **76** 3245
[115] Luo Z, Gao J, Djurisic A B, Yip C T and Zhang G B 2008 *Appl. Phys. Lett.* **92** 182501
[116] Jin K J, Lu H B and Zhou Q L 2005 *Phys. Rev. B* **71** 184428
[117] Sun J R, Shen B G and Tian H F 2005 *Appl. Phys. Lett.* **87** 202502
[118] Xiong C M, Zhao Y G and Xie B T 2006 *Appl. Phys. Lett.* **88** 193507
[119] Luo C, Jin K X, Chen C L and Wu T 2013 *Appl. Phys. Lett.* **103** 212401
[120] Wang J Y, Zhai W, Jin K X and Chen C L 2013 *Chin. Phys. Lett.* **30** 067301
[121] Jin K X, Zhai Y X, Li H, Tian Y F, Luo B C and Wu T 2014 *Solid State Commun.* **199** 39
[122] Sheng Z G, Nakamura M, Koshibae W, Makino T, Tokura Y and Kawasaki M 2014 *Nat. Commun.* **5** 4584
[123] Jin K X, Yang B and Zhang Y 2016 *Scr. Mater.* **112** 62
[124] Sonia, Patel R K, Kumar P, Prakash C and Agrawal D K 2012 *Ceram. Int.* **38** 1585
[125] Zhao S G, Zhang T, Liu W, Yan X L, Xie Y, Wang J Y and Jin K X 2014 *Physica B* **454** 42
[126] Wang J Y, Bai J Y, Xing H, Wang S H, Wang M, Jin K X and Chen C L 2017 *Solid State Commun.* **251** 35
[127] Zhao Y N, Luo B C, Chen C L and Jin K X 2017 *Phys. Status Solidi-Rapid Res. Lett.* **11** 1700155
[128] Zhao Y N, Luo B C, Xing H, Chen C L, Wang J Y and Jin K X 2017 *ACS Appl. Mater. Interfaces* **9** 6609
[129] Yan H, Wang J Y, Zhang Z T, Yang B, Chen C L and Jin K X 2017 *J. Appl. Phys.* **122** 115307
[130] Zhao S Z, Gu A, Yan X L, Han L M, Xie Y, Zhang T and Jin K X 2014 *Eur. Phys. Lett.* **108** 67007
[131] Jin K X, Zhang Y, Luo B C, Wang J Y, Chen C L and Wu T 2014 *Eur. Phys. Lett.* **103** 57007
[132] Zheng R K, Chao C, Chan H L W, Choy C L and Luo H S 2007 *Phys. Rev. B* **75** 024110
[133] Sheng Z G, Gao J and Sun Y P 2009 *Phys. Rev. B* **79** 174437
[134] Zhao Y Y, Wang J, Kuang H, Hu F X, Zhang H R, Liu Y, Zhang Y, Wang S H, Wu R R, Zhang M, Bao L F, Sun J R and Shen B G 2015 *Sci. Rep.* **4** 7075
[135] Wang J, Hu F X, Chen L, Zhao Y Y, Lu H X, Sun J R and Shen B G 2013 *Appl. Phys. Lett.* **102** 022423
[136] Zhao W, Zhang D, Meng D, Huang W and Feng L 2016 *Appl. Phys. Lett.* **109** 263502
[137] Zheng M and Wang W 2016 *J. Appl. Phys.* **119** 154507
[138] Wang J F and Gao J 2012 *Appl. Phys. Lett.* **100** 131903
[139] Jiang T, Wang X, Shen C, Wang X, Peng L, Fan L and Wu W 2016 *Appl. Phys. Lett.* **108** 113504
[140] Zarifi M, Kameli P, Ehsani M H, Ahmadv H and Salamati H 2016 *J. Magn. Magn. Mater.* **420** 33
[141] Tsui F, Smoak M C, Nath T K and Eom C B 2000 *Appl. Phys. Lett.* **76** 2421
[142] Wang J F, Jiang Y C, Wu Z P and Gao J 2013 *Appl. Phys. Lett.* **102** 071913
[143] Li W, Yan H, Chai X J, Wang S H, Dong X L, Ren L X, Chen C L and Jin K X 2017 *Appl. Phys. Lett.* **110** 192411
[144] Li W, Dong X L, Wang S H and Jin K X 2016 *Appl. Phys. Lett.* **109** 091907